

## Molecular-dynamics simulations of stress relaxation in metals and polymers

Slawomir Blonski\* and Witold Brostow

*Center for Materials Characterization and Department of Physics, University of North Texas, Denton, Texas 76203-5308*

Josef Kubát

*Department of Polymeric Materials, Chalmers University of Technology, S-412 96 Gothenburg, Sweden*

(Received 11 June 1993)

Molecular-dynamics simulations of stress relaxation have been performed for models of metals and polymers. A method that employs coupling between the simulation cell and an applied stress as well as an external thermal bath has been used. Two-dimensional models of the materials are defined with interactions described by the Lennard-Jones (Mie 6-12) and harmonic potentials. A special method is employed to generate chains in dense polymeric systems. In agreement with experiments, simulated stress-relaxation curves are similar for metals and polymers. At the same time, there exists an essential difference in the stress-strain behavior of the two kinds of simulated materials. During the relaxation, trajectories of the particles in different materials display a common feature: There exist domains in which movement of the particles is highly correlated. Thus, the simulation results support the cooperative theory of stress relaxation.

### I. INTRODUCTION

One often assumes that the responses of metals and polymers to external mechanical forces are vastly different. Actually, a similarity in the shape of stress-log time curves representing static stress relaxation in both polymers and metals had been established experimentally in 1965.<sup>1</sup> A cooperative theory was developed by Kubát to explain this phenomenon.<sup>2,3</sup> The theory has been able to reproduce successfully experimental stress-relaxation curves for polymers as well as for metals.<sup>4,5</sup>

The experimental findings are not only intriguing. Finding a reason or reasons for the similarities in stress-relaxation behavior in polymers and metals may be of considerable importance for the further development of advanced long-life materials.<sup>6,7</sup> This paper describes an attempt to gain new insights from molecular-dynamics simulations of stress relaxation in two-dimensional models of metals and polymers. Applied computer models of both polymers and metals are admittedly simplified; however, as will be shown in Sec. VII, they do exhibit all the essential features of these materials: The tensile-test curves obtained from the simulations of the two-dimensional models resemble those of the real three-dimensional materials.

Only pairwise interactions are used in these simulations. Although many-body interactions are often employed in simulations of materials,<sup>8</sup> the pair-potential approach has been found sufficient for a number of problems.<sup>9,10</sup> Therefore, it was used in earlier work when metals only were simulated.<sup>11</sup> For metals, all the interactions are treated equivalently, thus only one type of a pairwise potential is applied. For polymers, two kinds of pairwise potentials are used so as to include both bonding and nonbonding interactions. The connectivity, which is the existence of chain backbone's bonds in polymeric materials, constitutes the main difference between metals

and polymers. That difference, which is incorporated in the simulations, is much more important than details of the potential for nonbonding interactions.

### II. THE THEORY

The cooperative theory is described in Refs. 2–5. More recent papers deal with applications of the same approach to processes other than stress relaxation, including aging kinetics.<sup>12–14</sup> Key equations of the theory are quoted in an earlier paper,<sup>11</sup> hence now only the assumptions are briefly recalled. One supposes that a solid material is built up of structural units which behave as two-level systems; the upper state is occupied when the material is deformed. The stress relaxation is considered as a sequence of transitions from the higher to the lower level. Phonon interactions between the units cause the cooperativity of the relaxation process. However, the units in question are not specified in the theory in any particular way. Given the agreement between the experiment and the theory, and the simulation results for metals,<sup>11</sup> this situation behooves one to identify as much as possible the nature of the relaxing units. The similarity of behavior of metals and polymers suggests that some common features of the relaxing units in both kinds of materials might be expected.

### III. METHOD OF SIMULATIONS

Computer simulation runs have been carried out for an  $N$ -particle system placed in a rectangular simulation cell with periodic boundary conditions. A molecular-dynamics simulation technique is applied which allows the simulation cell to change size and orientation in response to any imbalance between internal and external stresses, and also provides control of the temperature of the sample. From various available methods,<sup>15</sup> the one

developed by Berendsen *et al.*<sup>16</sup> has been chosen. Advantages of that procedure, observed by Brown and Clarke,<sup>17</sup> were already confirmed:<sup>11,18</sup> The motion of the simulation cell is somewhat overdamped, hence there is little tendency for an unphysical oscillatory response to changes in the stress.

At the beginning of each time step of the simulations, updated velocities  $\mathbf{v}_i(t)$  are calculated for each particle using the formula

$$\mathbf{v}_i(t + \Delta t/2) = \mathbf{v}_i(t - \Delta t/2) + \frac{\mathbf{F}_i(t)}{m_i} \Delta t, \quad (1)$$

where  $t$  is the time,  $\Delta t$  is the time step of the molecular-dynamics simulation,  $\mathbf{F}_i(t)$  is the total force acting on the particle  $i$ , and  $m_i$  is the mass of the particle. The time step is taken to be  $\Delta t = 0.0075\sigma(m/\epsilon)^{1/2}$ . In this paper, the time and other physical variables are given in the system of *reduced units* appropriate for Lennard-Jones systems.<sup>15</sup> For additional simplicity, all the particles have equal masses and that mass is taken as a mass unit:  $m_i = 1m$ .

The new velocities computed from (1) are then scaled to maintain the constant temperature

$$\mathbf{v}'_i(t + \Delta t/2) = \lambda(t + \Delta t/2) \mathbf{v}_i(t + \Delta t/2), \quad (2)$$

where the coefficient  $\lambda(t)$  is given by

$$\lambda(t) = \{1 + \kappa_T [T_0/T(t) - 1]\}^{1/2}. \quad (3)$$

$\kappa_T$  is the rate of thermal relaxation which defines strength of coupling between the system and a "thermal bath." The value of  $\kappa_T = 0.05$  applied in the simulations guarantees that the coupling is sufficiently weak.  $T_0$  is the reference temperature. The system temperature  $T$  is obtained from kinetic energy  $E_k$  using the formula appropriate for a two-dimensional system:  $E_k = Nk_B T$ , where  $N$  is the number of particles in the system and  $k_B$  is the Boltzmann constant. The kinetic energy is calculated by the summation of squared velocities over all particles

$$E_k(t) = \frac{1}{2} \sum_{i=1}^N m_i v_i^2(t). \quad (4)$$

Updated coordinates of the particles  $\mathbf{r}_i(t)$  are found from the equation

$$\mathbf{r}_i(t + \Delta t) = \mathbf{r}_i(t) + \mathbf{v}'_i(t + \Delta t/2) \Delta t. \quad (5)$$

Then, the periodic boundary conditions are applied to the particle coordinates and the coordinates as well as the simulation cell are scaled using the equation

$$\mathbf{r}'_i(t + \Delta t) = \{\bar{1} + \kappa_0 [\bar{\sigma}_I(t) + \bar{\sigma}_E(t)]\} \mathbf{r}_i(t + \Delta t), \quad (6)$$

where  $\bar{1}$  is the unit tensor, and  $\bar{\sigma}_I(t)$  and  $\bar{\sigma}_E(t)$  are the tensors of the internal and external stress, respectively.

A convention is used such that in tension the external stress imposed on the material is positive, while the internal stress induced in the sample is negative. This is because, to balance the tension, these two stresses have to have the opposite directions. The coefficient  $\kappa_\sigma$  describes

the strength of coupling between the unbalanced stress and the size of the cell. The value  $\kappa_\sigma = 0.0005\sigma^2/\epsilon$  is used in the simulations. As already reported,<sup>11,18</sup> the system behaves very similarly for values of  $0.0004\sigma^2/\epsilon$  and  $0.000625\sigma^2/\epsilon$ . However, for  $\kappa_\sigma$  at least two times smaller or larger than  $0.0005\sigma^2/\epsilon$ , the cell turns out to be unstable and collapses.

The internal stress tensor is given by

$$\bar{\sigma}_i(t) = \frac{1}{V} \left[ \sum_{i=1}^N m_i \mathbf{v}_i \mathbf{v}_i - \sum_{i=1}^{N-1} \sum_{j=i+1}^N \mathbf{r}_{ij} \mathbf{F}_{ij} \right], \quad (7)$$

where  $\mathbf{r}_{ij}$  is the vector difference  $\mathbf{r}_i - \mathbf{r}_j$  evaluated using the periodic boundary conditions,<sup>19</sup> and  $\mathbf{F}_{ij}$  is the force acting on the particle  $i$  from the particle  $j$ .  $V$  is the volume (in the two-dimensional systems, the area) of the simulation cell. One realizes that not all the terms in the double summation are actually taken into account when the cutoff radius is used in the interactions between particles.

#### IV. INTERACTIONS

Pairwise interactions only are defined in the simulations. In the model of a metal, all the interactions are described by the Lennard-Jones (LJ) potential (which actually could be called the Mie 6-12 potential):<sup>20</sup>

$$U(r) = 4\epsilon \left[ \left( \frac{\sigma}{r} \right)^{12} - \left( \frac{\sigma}{r} \right)^6 \right], \quad (8)$$

where  $\epsilon$  and  $\sigma$  are the characteristic parameters of the potential, and  $r$  is the distance between two interacting particles. As discussed by Wang *et al.*,<sup>10</sup> parameters of the potential can be chosen so as to correspond to a real material (such as copper). The cutoff radius for the LJ interactions is used at the distance of  $2.5r_0$ , where  $r_0 = 2^{1/6}\sigma$ . Thus, two shells of neighbors (immediate and second-nearest) around a given atom (in metal) or a chain segment (in polymer) are taken into account. In the polymer, there is additionally the connectedness of particles along the macromolecular backbone. The respective *intra*chain interactions are described instead by a harmonic potential

$$V(r) = K \left[ \frac{r}{r_0} - 1 \right]^2 \quad (9)$$

with the constant  $K$  specifying strength of this bonding interactions. The value  $K = 20\epsilon$  was chosen to have similar kinetics of stress relaxation both in metals and in polymers. This facilitates comparisons without affecting the fundamental differences between metals and polymers.

Using only two potentials to define the interactions in polymers might appear to be an oversimplification. However, such models have been successfully used to study polymers.<sup>21</sup> Moreover, even when the distance of the minimum in the LJ potential ( $r_0$ ) is defined to be equal to the bond length, the stress-strain curves of the models suggestively display characteristic features of real metals and polymers. These features are discussed in more detail in the following sections.

## V. INITIAL CONFIGURATIONS

In the simulations of metals, the particles are initially placed on a two-dimensional hexagonal lattice with a nearest-neighbor distance of  $r_0$ . In the beginning all the lattice sites in the simulation cell are occupied. Then a number of vacancies is generated in the sample. Randomly chosen particles are moved from the interior of the sample to an additional layer (or more additional layers when needed) of the sites located at a side of the cell. In all the simulations, regardless the size of the system, the same fraction ( $\frac{1}{30}$ ) of the total number of particles is moved.

The system is then equilibrated without an external stress applied. First, the simulation runs for  $5000\Delta t$  at the temperature  $T=0.4\epsilon/k_B$ , which is somewhat below the melting temperature of such a LJ system.<sup>9,11,22,23</sup> Next, the system is equilibrated for  $25\,000\Delta t$  at a lower temperature—chosen for performing stress-strain and stress-relaxation numerical experiments. Although the starting configuration is initially constructed on the lattice, the procedure of the equilibration ensures that the configuration is appropriate for the off-lattice molecular-dynamics simulations.

Models of polymers are prepared in a similar way, but before the equilibration the particles are connected into one chain using the algorithm described in Sec. VI. Vacancies are also introduced into the polymers. The vacancies contribute to the free volume in the sample, rendering the simulated system much more realistic. The importance of free volume for mechanical properties of polymeric materials has been discussed earlier.<sup>6,7,24</sup> Figure 1 shows two exemplary configurations of the metal and the polymer that were equilibrated at the temperature  $T=0.2\epsilon/k_B$ .

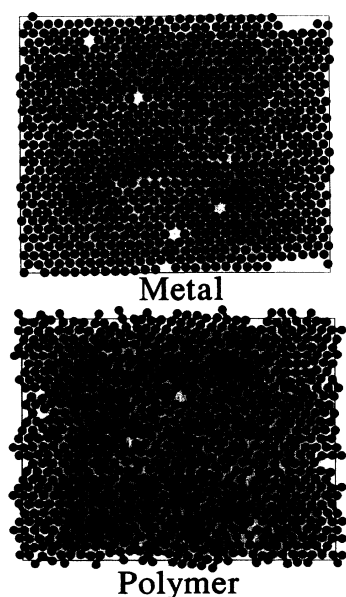


FIG. 1. Sample configurations of the 900-particle models of metals and polymers. The circle diameters are taken to be  $\sigma$ .

## VI. POLYMER GENERATION

It is not easy to generate an off-lattice model of a bulk polymer system which has density comparable to the density of the completely filled lattice. Successful attempts to generate three-dimensional lattice models with all the sites occupied have been reported by Pakula.<sup>25,26</sup> A different method of construction of a self-avoiding chain on the two-dimensional lattice has been developed by Mom.<sup>27</sup> The Mom approach is used in this work to generate one polymer chain from particles placed on the hexagonal lattice. Although there are vacancies in the system, they are not necessary to obtain the chain. The method works as well for the completely filled lattices. One can also expect that the method may be used to generate systems of many chains. Therefore, it is reasonable to proceed via generation of the on-lattice polymer, followed by the off-lattice molecular-dynamics equilibration, as a method to obtain starting configurations for simulations of the dense polymeric systems.

In the beginning of the chain generation, all the particles constitute “chains” of one particle each. Using the graph theory concepts (for a brief account see Sec. 2.2 in Ref. 20),<sup>28</sup> we thus start with walks of the length equal to zero. The main step of the generation consists in finding two chains in which an end particle of one of the chains is the nearest neighbor of an end particle of the other chain. When such chains are found, they become connected and form one longer chain. Thus, the number of chains in the system decreases by one. The main step is repeated until only a single chain remains. The process is easy at the beginning, but its difficulty increases as the number of chains decreases. At some point, there are no more chains which can be connected in this way.

To allow for further chain development, the end particles have to be changed. As proposed by Mom, the system is then scanned to see whether there is a particle inside one of the chains that is the nearest neighbor of one of the end particles of another chain. When such a particle is found, a part of the former chain is connected with the latter. The number of chains does not decrease in this process, but the lengths of both chains change and new particles appear on their ends. However, because there is a possibility that the improvement process can fall into an infinite loop, a random choice is made as to whether a rearrangement should be accepted for the particle so found. If the change is done, then the main step of the generation process can be repeated.

For large systems such as those containing 3600 particles, there is a possibility, not taken into account by Mom, that for all chains the end particles are surrounded by particles belonging to the same chain. In such a case the improvement procedure described above is useless. Then, a particle is sought that is the nearest neighbor of the end particle of the same chain, but is not yet bounded to the chain end. When such a particle is found, the chain is rearranged and a new particle appears on its end. The decision to apply the change is also taken at random, but when the change is done, the main step of the generation process can be repeated once more.

The chain generation process requires many operations to be done. For example, there were 2860 and 18 532

iterations needed to generate the chains of 900 and 3600 particles, respectively.

## VII. RESULTS

All the simulations of stress relaxation have been performed with the initial strain of 10% applied in the direction of one side of the sample. Thus, the deformation is made in the direction parallel to one of the crystallographic planes of the initial hexagonal lattice. The strain in the material is measured using changes in the size of the simulation cell. During the simulation, such an external stress is applied that the strain in the direction in which it was initially applied remains constant. The internal stress in the direction of the applied strain is reported as the stress in the material.

Many test simulations were run to verify the method employed. Dependence of the results on the system size seems to be the most important problem, but it was found that results of the stress-relaxation simulations do not depend significantly on the number of particles in the system. Figure 2(a) shows the results of the simulations conducted for the model of metal at the temperature  $T=0.20\epsilon/k_B$ . The curves are suggestively similar, despite the large differences in the system size. This shows convincingly that the simulations correspond to a

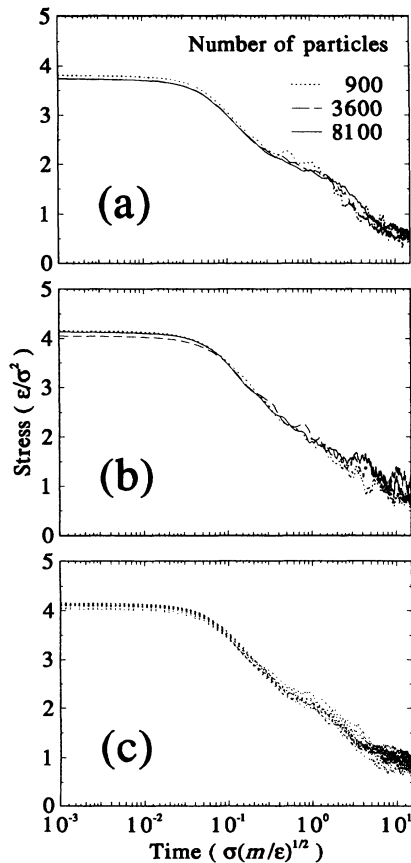


FIG. 2. Simulated stress-relaxation curves obtained for (a) metals with different number of particles in the system (b) three metals with different initial configurations, and (c) for ten different configurations of the 3600-particle polymer chain.

physical reality, this even if the smooth parts of the curves correspond to less than 50 initial time steps of the molecular-dynamics simulation. The simulated stress-relaxation process is accompanied by contraction of the material. This indicates a positive Poisson ratio, the usual feature of real materials.<sup>20</sup>

In other tests, the dependence of the simulated stress-relaxation curves on the initial configuration of the system was studied. Stress-relaxation curves obtained for three different initial configurations of the metal are shown in Fig. 2(b). Because the curves are not significantly different, one infers that a limited number of the initial configurations is sufficient. For the model of polymers, ten chains with different configurations of 3600 particles each were generated and fully relaxed in the way described above. Stress-relaxation simulations were then performed for all of the polymers. Results are shown in Fig. 2(c). The curves are very similar and give an apparent average. The averaging over the chain configurations allows for smoothing of the stress-relaxation curves for longer times.

The simulations were performed for the temperatures 0.1, 0.2, and  $0.3\epsilon/k_B$ . If one takes  $\epsilon=2.5\times 10^{-20}$  J, which is an appropriate value for metals,<sup>10</sup> then these temperatures correspond to the real temperatures of 181, 362, and 543 K, respectively. The results for metals are shown in Fig. 3. At the lowest temperature, the stress induced in the sample by the applied strain is the largest and its relaxation is the slowest. With the increasing temperature, the initial stress decreases and the relaxation rate increases. The present results complement in an important way those in Ref. 11.

Choosing an appropriate strength of the bonding interactions in the model of a polymer, it was possible to obtain in the simulations similar rates of stress relaxation in metals and polymers. Although the stress-relaxation curves are similar, *not all* mechanical properties of the different materials are the same. The simulations of tensile tests show that the model of a polymer displays behavior characteristic for real polymeric materials. By contrast, the model of a metal behaves quite differently. In the simulations of stress-strain experiments, uniaxial stress is applied at the constant rate  $\Delta\sigma/\Delta t=0.018(\epsilon^3/m)^{1/2}/\sigma^3$ . The rate as well as the time step have been chosen equal to the values used in

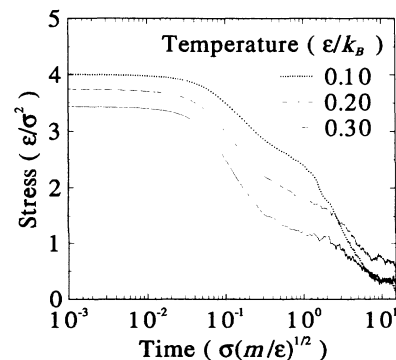


FIG. 3. Temperature dependence of stress relaxation in the 8100-particle model of a metal.

Ref. 10, to allow for comparison of the results. Stress-strain curves obtained from the simulations are presented in Fig. 4. The curve for the polymer is an average from the curves obtained for ten chains with different configurations.

One sees in Fig. 4 that the stresses increase from zero up to the tensile strength. From that point, the behavior of the two materials is dramatically different. In the metal the stress decreases monotonically after failure. In the polymer, however, fracture does not occur yet. There is a "plateau" in the stress-strain curve followed by a stress increase. This behavior is typical for polymeric materials. Note that, drawing only parts of the curves in another scale, it was possible to recover Fig. 1(b) from Ref. 10. The only difference is that in the present simulations the oscillations are *not* observed. This shows that the stress-strain curves obtained here are typical for such models of materials.

Comparison of the average stress-relaxation curves is presented in Fig. 5(a). Subsequent configurations of the particles, obtained during the simulations of stress relaxation, have been analyzed using the concept of the Voronoi network.<sup>29-31</sup> Tessellation of the two-dimensional space into Voronoi polygons has been done using the procedure provided by Allen and Tildesley.<sup>15</sup> Figure 5(b) shows the fractions of the Voronoi hexagons in the models of metals and polymers during the simulations of stress relaxation. The fraction of the six-side polygons is used as a measure of the lattice deformation. For an ideal hexagonal lattice, that fraction is equal to one, while for a defective lattice it is less than one. The simulations show that the difference is mainly due to polygons with five and seven sides. Such polygons are formed near lattice defects. Comparison of Fig. 5(b) with Fig. 5(a) shows that the central descending part of the relaxation curve corresponds to *defect formation*. This becomes visible particularly in the second part of that central period when the fraction of hexagons decreases. The last part of the stress-relaxation curve, that is tending towards the internal stress value, has a significance at the atomic level: a *rearrangement* of the structure takes place, because the system tries to obliterate effects of the changes

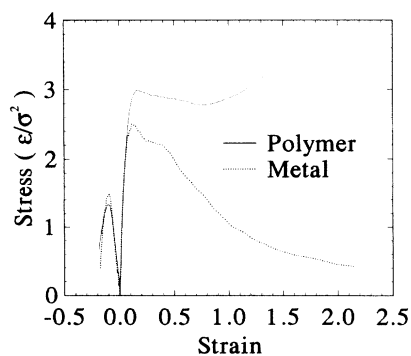


FIG. 4. Stress-strain curves obtained from the simulations of the 3600-particle materials at the temperature  $T=0.20\epsilon/k_B$ . The curves for negative and positive strain are, respectively, for the stress measured in the direction perpendicular and parallel to the applied stress.

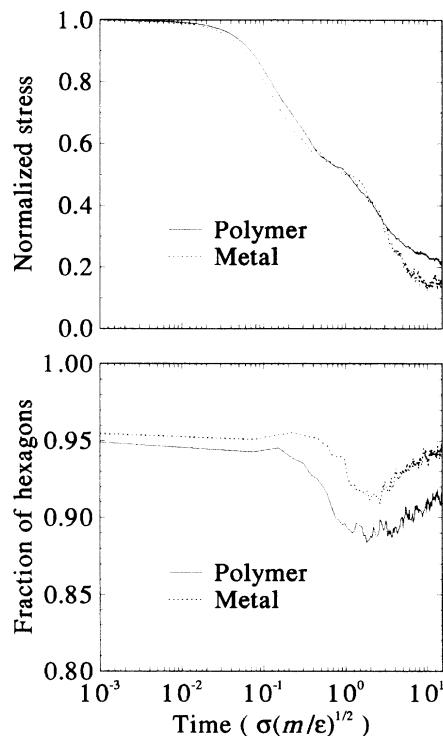


FIG. 5. (a) Comparison of stress relaxation in simulations of 3600-particle models of metals and polymers at  $T=0.20\epsilon/k_B$ . (b) Fraction of the hexagonal Voronoi polygons in the samples during the stress-relaxation simulations.

brought from the outside. The reformation results in an increase of the fraction of hexagons; that increase, however, is necessarily insufficient for reaching the original value before the strain imposition.

Figure 6 shows trajectories of the particles during the initial 50 time steps of the molecular-dynamics simulations of stress relaxation in the models of metals and polymers. The similarity of the pictures is apparent. In both the metals and the polymers, there occur domains in which movement of the particles is highly correlated. The domains have similar shapes, forced by the symmetry of the lattice, but they have different sizes. Such domains are essentially induced by the strain applied to the samples: The particles move in the correlated way—so as to adjust to the new volume of the strained sample. The domains observed here clearly correspond to clusters envisaged earlier in the cooperative theory.<sup>2-5</sup>

Abraham has found similar domains in the LJ system near the melting point—when the system has been intermittently changing between the solid and the liquid state.<sup>32,33</sup> Since the phase transition is accompanied by a change in the volume of the sample a thermal strain is created in the material. This is similar to a thermal stress created by a temperature gradient. It is known that a thermal stress causes deformation—with similar consequences as a mechanical stress field (see Section 12.4 in Ref. 20). By contrast, in unstrained LJ systems in the solid state the formation of such domains has not been observed.<sup>22,23,34-36</sup>

The present simulations of two-dimensional systems re-

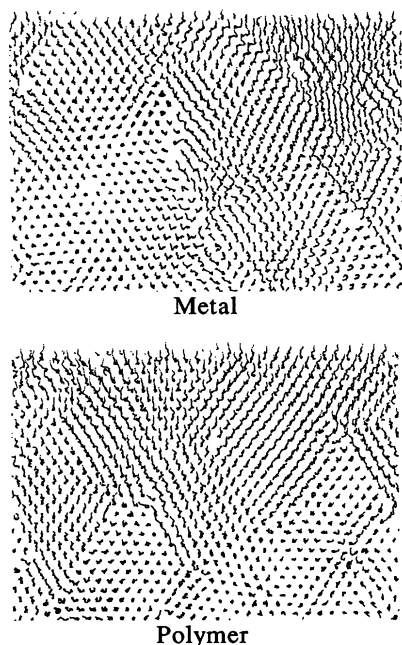


FIG. 6. Trajectories of the particles obtained from the first 50 time steps of the simulations at  $T=0.20\epsilon/k_B$ .

sult in stress-relaxation curves which have all the essential features of curves obtained from experiments on three-dimensional materials. Consider for instance two six-particle clusters or domains: one planar, and the other with two particles in the central plane, two above and two below. The stress-relaxation curve is a consequence of numerous domain relaxation events, with domains perhaps such as defined above, plus in various other

shapes (and sizes). Apparently, the shapes—and even dimensionalities—of individual domains do not matter for the relaxation process.

### VIII. CONCLUSIONS

The method and the results of molecular-dynamics simulations of stress relaxation in models of metals and polymers have been presented. There is a large difference in the *stress-strain behavior* of the models, and in both cases the essential features known from experiments appear also in the simulated diagrams. Simultaneously, the time dependence of the *stress relaxation* for metal and polymer models is similar. This is also in agreement with the experimental results.<sup>1</sup> The spatial domains observed in the pictures of the trajectories of particles may be interpreted as the relaxation units assumed to exist in the general cooperative theory of stress relaxation in materials.<sup>2-5, 12-14</sup> As assumed in the theory—and now confirmed by the simulations—each relaxing unit consists of several particles. The simulations thus show the existence of relaxing clusters as the common denominator in stress relaxation behavior of different classes of materials. Apparently, it is not very significant whether such a cluster consists of metal atoms or of polymer chain segments.

Simulations show also other features in common with the theory and also with experiments. One recalls the result in Ref. 11 that the slope of the linear part of the relaxation curve is proportional to the initial effective stress. Highly important are the results of the simulations at different temperatures. Since experimental results for a single material at several temperatures are rare, data presented in Fig. 3 are useful for prediction of experimental stress-relaxation diagrams.

\*On leave from the Department of Applied Physics, Technical University of Gdansk, 80-952 Gdansk, Poland.

<sup>1</sup>J. Kubát, *Nature (London)* **205**, 378 (1965).

<sup>2</sup>Ch. Högfors, J. Kubát, and M. Rigdahl, *Phys. Status Solidi B* **107**, 147 (1981).

<sup>3</sup>J. Kubát, *Phys. Status Solidi B* **111**, 599 (1982).

<sup>4</sup>J. Kubát, L.-Å Nilsson, and W. Rychwalski, *Res. Mech.* **5**, 309 (1982).

<sup>5</sup>J. Kubát and M. Rigdahl, in *Failure of Plastics*, edited by W. Brostow and R. D. Corneliussen (Hanser, Munich, 1986).

<sup>6</sup>W. Brostow, in *Failure of Plastics*, Ref. 5.

<sup>7</sup>W. Brostow, *Makromol. Chem. Macromol. Symp.* **41**, 119 (1991).

<sup>8</sup>*Atomistic Simulation of Materials: Beyond Pair Potentials*, edited by V. Vitek and D. J. Srolovitz (Plenum, New York, 1989).

<sup>9</sup>K. Toukan, F. Carrion, and S. Yip, *J. Appl. Phys.* **56**, 1455 (1984).

<sup>10</sup>Z.-G. Wang, U. Landman, R. L. Blumberg Selinger, and W. M. Gelbart, *Phys. Rev. B* **44**, 378 (1991).

<sup>11</sup>W. Brostow and J. Kubát, *Phys. Rev. B* **47**, 7659 (1993).

<sup>12</sup>M. J. Kubát, J.-F. Jansson, M. Delin, J. Kubát, R. W. Rychwalski, and S. Uggla, *J. Appl. Phys.* **72**, 5179 (1992).

<sup>13</sup>D. G. Kubát, H. Bertilsson, J. Kubát, and S. Uggla, *Rheol.*

*Acta.* **31**, 390 (1992).

<sup>14</sup>D. G. Kubát, H. Bertilsson, J. Kubát, and S. Uggla, *J. Phys. Condens. Matter* **4**, 7041 (1992).

<sup>15</sup>M. P. Allen and D. J. Tildesley, *Computer Simulation of Liquids* (Clarendon, Oxford, 1990).

<sup>16</sup>H. J. C. Berendsen, J. P. M. Postma, W. F. van Gunsteren, A. DiNola, and J. R. Haak, *J. Chem. Phys.* **81**, 3684 (1984).

<sup>17</sup>D. Brown and J. H. R. Clarke, *Macromolecules* **24**, 2075 (1991).

<sup>18</sup>S. Blonski, W. Brostow, and J. Kubát, *Makromol. Chem. Macromol. Symp.* **65**, 109 (1993).

<sup>19</sup>A. J. C. Ladd, in *Computer Modelling of Fluids, Polymers and Solids*, edited by C. R. A. Catlow, S. C. Parker, and M. P. Allen (Kluwer, Dordrecht, 1990).

<sup>20</sup>W. Brostow, *Science of Materials* (Wiley, New York, 1979).

<sup>21</sup>Yu. Ya. Gotlib, N. K. Balabaev, A. A. Darinskii, and I. M. Neelov, *Macromolecules* **13**, 602 (1980).

<sup>22</sup>F. F. Abraham, *Phys. Rev. Lett.* **44**, 463 (1980).

<sup>23</sup>F. F. Abraham, *Phys. Rep.* **80**, 339 (1981).

<sup>24</sup>W. Brostow, M. Fleissner, and W. F. Müller, *Polymer* **32**, 419 (1991).

<sup>25</sup>T. Pakula, *Polymer* **28**, 1293 (1987).

<sup>26</sup>T. Pakula, *Macromolecules* **20**, 679 (1987).

- <sup>27</sup>V. Mom, *J. Comput. Chem.* **2**, 446 (1981).
- <sup>28</sup>F. Harary, *Graph Theory* (Addison-Wesley, Reading, MA, 1969).
- <sup>29</sup>W. Brostow, J.-P. Dussault, and B. L. Fox, *J. Comput. Phys.* **29**, 81 (1978).
- <sup>30</sup>V. Krishnamurthy, W. Brostow, and J. S. Sochanski, *Mater. Chem. Phys.* **20**, 451 (1988).
- <sup>31</sup>N. N. Medvedev, A. Geiger, and W. Brostow, *J. Chem. Phys.* **93**, 8337 (1990).
- <sup>32</sup>F. F. Abraham, *Phys. Rev. Lett.* **50**, 978 (1983).
- <sup>33</sup>S. W. Koch and F. F. Abraham, *Phys. Rev. B* **27**, 2964 (1983).
- <sup>34</sup>S. Toxvaerd, *Phys. Rev. Lett.* **44**, 1002 (1980).
- <sup>35</sup>F. F. Abraham, *Rep. Prog. Phys.* **45**, 1113 (1982).
- <sup>36</sup>K. J. Strandburg, *Rev. Mod. Phys.* **60**, 161 (1988).